

Systematic Survey on Heavy-residue Production in Fragmentation Reactions

T. Enqvist*, P. Armbruster[†], J. Benlliure**, M. Bernas[‡], A. Boudard[§], E. Casarejos**, S. Czajkowski[¶], R. Legrain[§], S. Leray[§], B. Mustapha[‡], J. Pereira**, M. Pravikoff[¶], F. Rejmund[‡], K.-H. Schmidt[†], C. Stéphan[‡], J. Taieb[‡], L. Tassan-Got[‡], F. Vivés[†], C. Volant[§] and W. Wlaził[§]

*University of Jyväskylä, Department of Physics, P.O. Box 35, FIN-40351 Jyväskylä, Finland

[†]GSI, Planckstraße 1, D-64291 Darmstadt, Germany

**Universiad de Santiago de Compostela, E-15706 Santiago de Compostela, Spain

[‡]IPN Orsay, IN2P3, F-91406 Orsay, France

[§]DAPNIA/SPhN CEA/Saclay, F-91191 Gif sur Yvette, France

[¶]CENBG, IN2P3, F-33175 Gradignan, France

Abstract.

The production cross sections and the kinematical properties of primary residual nuclei have been studied in reactions $^{197}\text{Au} + \text{p}$, $^{208}\text{Pb} + \text{p,d}$, $^{238}\text{U} + \text{p,d}$, and $^{238}\text{U} + ^{208}\text{Pb}$ at energies around 1 A GeV. The measured kinematical properties of the residues were also used to disentangle the relevant reaction mechanisms, spallation-evaporation and spallation-fission. The fragment separator FRS at GSI, Darmstadt, was used to separate and identify the reaction products.

The measured quantities are important for the design of accelerator-driven subcritical reactors and for the planning of future radioactive-beam facilities.

INTRODUCTION

A project has been started at GSI to determine primary residue production cross sections down to 0.1 mb, aiming at accuracies of 10%, and their kinematical properties for a series of spallation or fragmentation reactions. The reactions studied include ^{197}Au (0.8 AGeV) + p, ^{208}Pb (1 AGeV) + p,d, ^{238}U (1 AGeV) + p,d, and ^{238}U (1 AGeV) + ^{208}Pb [1, 2, 3, 4, 5, 6, 7, 8]. For some of the systems (^{238}U (1 AGeV) + p,d) only a part of the measured data has been analysed. In addition, the analysis of the data for systems ^{56}Fe , ^{60}Ni (0.3... 1.5 AGeV) + p,d is in progress.

The data are relevant for estimating the intensities available in next-generation radioactive-beam facilities [9], and for the evaluation of the radiotoxicity in accelerator-driven subcritical reactors which are proposed for incinerating nuclear waste [10, 11] and/or for producing energy [12].

Up to very recently, all our knowledge on isotopic cross sections of heavy residues from spallation reactions of high-energy protons with heavy nuclei relied on radiochemical methods and mass spectrometry (e.g. [13, 14, 15, 16, 17, 18, 19]). These techniques gave access to long-lived residues only, and thus mainly cumulative yields were determined, resulting from beta decay of the primary reaction products. Instead of using the former techniques, it has become possible to have access to all produced primary residues by using inverse kinematics by bombarding a liquid-hydrogen target with relativistic heavy ions. The reaction products are identified in-flight in atomic number and in mass using a recoil separator. In addition to the determination of production cross sections, this technique is also able to give information on the reaction kinematics and the velocities of the reaction products.

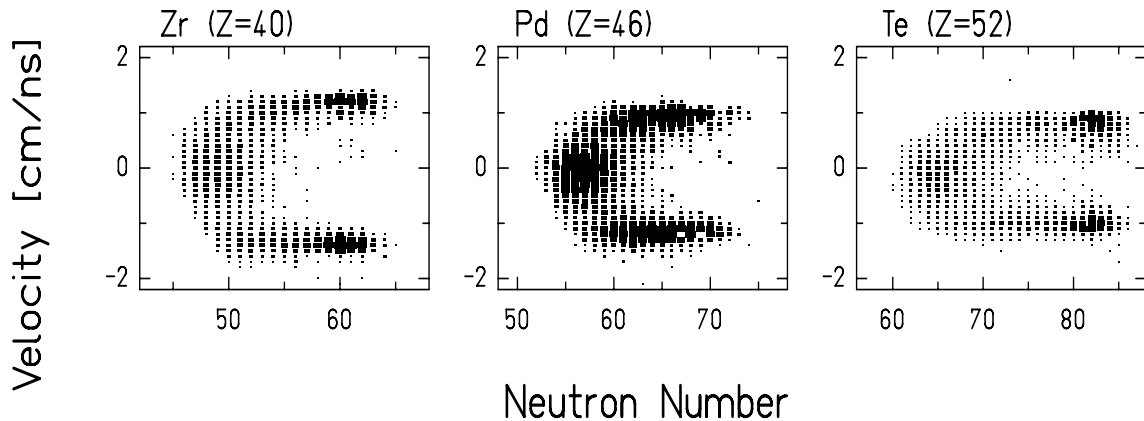


FIGURE 1. Two-dimensional cluster plots of velocity versus neutron number are shown for 3 selected elements from the reaction ^{238}U (1 AGeV) + ^{208}Pb . The velocity is given in the centre-of-mass system of the primary beam in the middle of the target. The more neutron-rich isotopes are produced by fission and the more neutron-deficient by fragmentation. In between, there is a mixture from both of the production mechanisms.

EXPERIMENT AND DATA ANALYSIS

The experiments were performed at GSI in Darmstadt, Germany. The heavy-ion synchrotron SIS delivered the primary beam and reaction products were separated and identified by using the fragment separator FRS [20] and associated detector equipments. The FRS is a two-stage magnetic spectrometer with a dispersive intermediate image plane (S_2) and an achromatic final image plane (S_4). Position-sensitive plastic-scintillation detector placed at S_2 and S_4 provided the magnetic rigidities and the time-of-flight measurements. The primary-beam intensity was continuously monitored and measured with the beam-current monitor SEETRAM from the current induced by secondary electrons in 3 aluminium foils of a total thickness of 8.9 mg/cm^2 .

Depending on the atomic number of a reaction product, the measurement and identification in atomic and mass numbers was done in different ways. For reaction products closer to the primary beam, i.e. heavier residues, a profiled aluminium degrader, of thickness around 5 g/cm^2 , which preserves the achromacy of the spectrometer was installed at S_2 of the FRS in order to achieve the necessary nuclear-charge resolution. The Z and A were identified by plotting the horizontal position at S_4 versus A/Q of reaction products for each setting. The elements below $Z \sim 65$ were identified using an ionisation chamber, and the degrader was removed from the beam-line. By knowing the time-of-flight, magnetic rigidity and atomic number, the mass number could be calculated.

The velocity of a residue identified in Z and A was then determined from the $B\rho$ value now obtained from the horizontal position at S_2 . The velocity was then transformed into the reference frame of the primary beam in the middle of the target by Lorentz transformation, taking into account the appropriate energy loss. In Fig. 1, the velocity distributions are shown for 3 selected elements from the reaction ^{238}U (1 AGeV) + ^{208}Pb . The size of the symbol is proportional to the production rate of the isotope. It can be seen from the distributions that the reaction products can be attributed to different reaction mechanisms, i.e. spallation-fission and spallation-evaporation.

The production rates in Fig. 1 has been corrected for dead time of the data-acquisition system, for the contribution from incompletely stripped ions, and for counting losses due to secondary reactions in the scintillation detector at S_2 . It is also normalised to the number of projectiles N_p recorded by the beam-intensity monitor. In order to get final cross section values, additional corrections on the production rates include corrections for angular transmission of the FRS and secondary reactions inside the target.

For more detailed explanations on the experimental method and data analysis, see Refs. [1, 2, 3, 4, 5, 6, 7, 8].

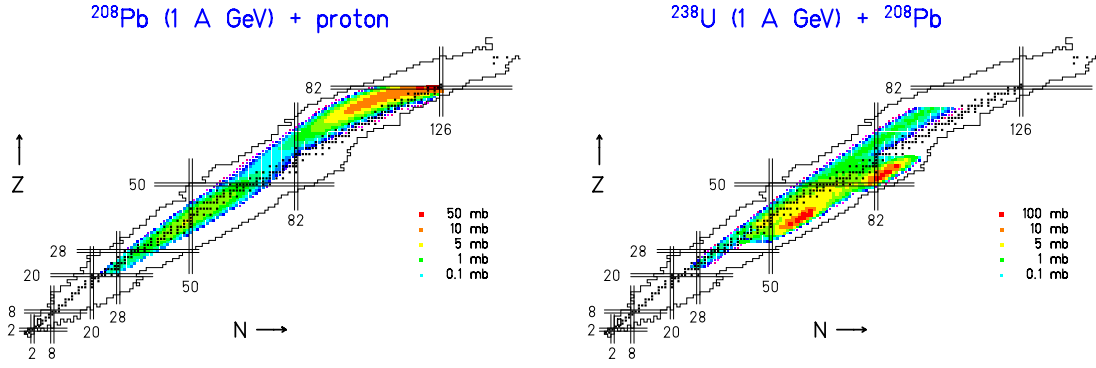


FIGURE 2. Two-dimensional cluster plots of the isotopic production cross sections obtained in the reactions ^{208}Pb (1 A GeV) + p and ^{238}U (1 A GeV) + ^{208}Pb .

RESULTS

The measured production cross sections of the two systems, ^{208}Pb (1 A GeV) + p and ^{238}U (1 A GeV) + ^{208}Pb , have been summarised in Fig. 2 as a form of chart of the nuclides. The experiment of the latter reaction was only sensitive to elements between vanadium and rhenium, and lightest and heaviest residues produced in the reaction are not shown in Fig. 2.

The total reaction cross section for the reaction ^{208}Pb (1 A GeV) + p determined by the projection from the full mass distribution was measured as $\sigma_{\text{tot}} = (1.99 \pm 0.27)$ b, and calculated to be $\sigma_{\text{tot}} = 1.80$ b using the Glauber-type calculation as described in Ref. [21] with realistic nuclear-density distributions. For the reaction ^{208}Pb (1 A GeV) + d the total reaction cross section was determined to be $\sigma_{\text{tot}} = (2.28 \pm 0.26)$ b which also agrees well with the result of a Glauber-type calculation giving $\sigma_{\text{tot}} = 2.32$ b. Both of the reactions produce around 1000 isotopes above 0.1 mb.

In the reaction ^{197}Au (0.8 A GeV) + p the total reaction cross section of $\sigma_{\text{tot}} = (1.6 \pm 0.2)$ b was measured.

The total fission cross section in the reaction ^{238}U (1 A GeV) + ^{208}Pb , evaluated from the sum of the individual isotopic cross sections of fission products, amounted to $\sigma_{\text{fis}} = (3.9 \pm 0.6)$ b. The total reaction cross section, or the total fragmentation cross section, of the reaction ^{238}U (1 A GeV) + ^{208}Pb could not be determined since the experiment wasn't sensitive to the elements lighter than vanadium and heavier than rhenium, due to the time restrictions.

The mean longitudinal momentum and the standard deviation of the momentum distribution of any isotope could be determined from the corresponding measured velocity distributions by using the non-relativistic equations since velocities were transformed into the center-of-mass system.

Fig. 3 shows the average mean values and standard deviations of the momentum distributions of spallation residues as a function of mass number from reactions ^{208}Pb (1 A GeV) + p as open symbols and ^{208}Pb (1 A GeV) + d as full symbols. The data are compared with the empirical systematics proposed by Morrissey [22] as the solid line, and with the predictions of the Goldhaber model [23] as the dashed line. The average mean value and the width of the longitudinal-momentum distribution were taken as weighted mean by using the production cross section of the isotope as a weighting factor.

DISCUSSION

The total fission cross sections of the reactions ^{208}Pb (1 A GeV) + p and ^{208}Pb (1 A GeV) + d are almost identical, and the increase of the total reaction cross section in the reaction ^{208}Pb + d compared to the reaction ^{208}Pb + p is due to the more abundant production of medium-heavy residues ($A \sim 150 - 170$) in ^{208}Pb + d reactions. The measured total reaction cross sections of these two reactions are in good agreement with the results of the model of Karol.

The total fission cross section of the reaction ^{238}U (1 A GeV) + ^{208}Pb ($\sigma_{\text{fis}} = (3.9 \pm 0.6)$ b) can be compared to the result of Hesse et al. [24] who obtained a cross section of $\sigma_{\text{fis}} = (3.54 \pm 0.21)$ b at 750 A MeV beam energy. Due to a slightly higher beam energy in our work, a slightly higher electromagnetic-induced fission cross section is expected,

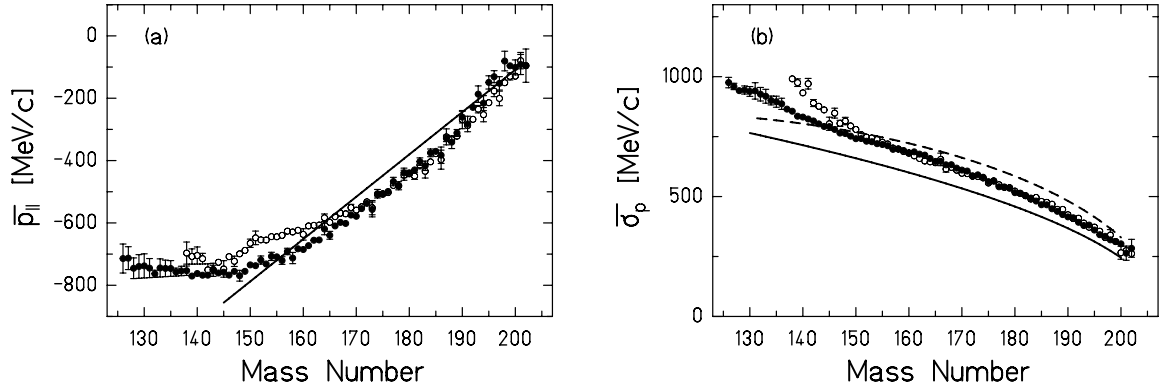


FIGURE 3. Average mean values (a) and standard deviations (b) of the momentum distribution of spallation residues induced in the reactions of ^{208}Pb (1 A GeV) + p (open symbols) and ^{208}Pb (1 A GeV) + d (full symbols). The solid line indicates the empirical systematics derived by Morrissey [22] for the mean value and the width, respectively, and the dashed line the predictions of the Goldhaber model [23].

and in view of the experimental errors, our data are in good agreement with Ref. [24].

The comparison of the momentum distribution of spallation-evaporation residues between the reactions ^{208}Pb (1 A GeV) + p and ^{208}Pb (1 A GeV) + d is shown in Fig. 3(a) and (b). It can be seen that the average mean longitudinal momentum and standard deviation of the distribution are essentially identical between the two reactions.

The average mean values agree well with the experimental systematics of Morrissey in Fig. 3(a) at heavier masses. At lighter masses there starts to be a clear deviation from the straight-line systematics of Morrissey. There already exists previous evidence for a deviation from the Morrissey systematics with decreasing mass number. The data of Fig. 3 indicate a saturation in the longitudinal momentum at small masses ($A \sim 130 - 150$). Since there is no production of spallation-evaporation residues below $A \sim 125$ in the reactions ^{208}Pb (1 A GeV) + p and ^{208}Pb (1 A GeV) + d, it is difficult from these data to predict the behaviour at the lighter masses.

The design of an accelerator-driven system requires a precise knowledge of the production cross sections and energies of residues inside the spallation target. From the production cross sections of long-lived isotopes, for example, it is possible to estimate the level of the long-term radiotoxicity problem of the target. On the other hand, short-lived activities may be responsible for maintenance problems.

The data may also provide valuable information on the production of radioactive beams. One of the main interests in developing methods for producing radioactive beams, is to have an access to neutron-rich isotopes. Low-energy fission of heavy elements (uranium or thorium) has been considered as a production method for the element range from zinc to neodymium by projectile fragmentation or proton-induced reactions. It can be seen from Fig. 2 that fission products from the reaction of 1 GeV protons on lead are very much concentrated close to the stable nuclei, and not on the neutron-deficient nor the neutron-rich side. In the reaction ^{238}U (1 A GeV) + ^{208}Pb , on the contrary, the main contribution comes from the electromagnetic-induced low-energy fission. Thus, the use of lead is not a good choice to produce neutron-rich radioactive beams in the medium-Z region. A similar conclusion can also be made for the reaction 0.8 GeV protons on gold and 2 GeV deuterons on lead. These reactions investigated can, however, be utilised for producing neutron-rich radioactive beams of heavier elements closer to the projectile by spallation (projectile fragmentation), see Ref. [25].

CONCLUSION

The full isotopic distributions of spallation-fission and spallation-evaporation residues of the reactions ^{197}Au (0.8 A GeV) + p, ^{208}Pb (1 A GeV) + p,d, ^{238}U (1 A GeV) + p,d, and ^{238}U (1 A GeV) + ^{208}Pb were measured for the first time. The use of the inverse kinematics together with the in-flight separator FRS at GSI seems to be the optimal technique to identify all the primary residues in the atomic and mass number, and to determine their production cross sections

and kinematical properties with high accuracy.

The data, production cross sections and energies, are of highest interest for the design of accelerator-driven systems. Using the measured production cross sections, combined with the known decay properties, the short- and long-term radioactivities in the target material can be calculated. The number of atomic displacements being the reason for radiation damages in the structural materials can now be estimated from the measured momentum (or kinetic-energy) distributions.

It was seen that the electromagnetic-induced fission of the reaction ^{238}U (1 A GeV) + ^{208}Pb could be well suited for the production of neutron-rich fission fragments in the next-generation radioactive-beam facilities. A conclusion was made that the reactions ^{197}Au (0.8 A GeV) + p and ^{208}Pb (1 A GeV) + p are not optimal to produce neutron-rich isotopes in the fission-fragment element range. On the other hand, this reaction is a good candidate to produce very neutron-rich isotopes of heavier elements closer to the projectile.

REFERENCES

1. T. Enqvist et al., Nucl. Phys. A 658 (1999) 47.
2. W. Wlazio et al., Phys. Rev. Lett. 84 (2000) 5736.
3. J. Benlliure et al., Nucl. Phys. A 683 (2001) 513.
4. F. Rejmund et al., Nucl. Phys. A 683 (2001) 540.
5. T. Enqvist et al., Nucl. Phys. A 686 (2001) 481.
6. T. Enqvist et al., to be submitted to Nucl. Phys. A.
7. J. Taieb, Ph.D. Thesis, Universite de Paris-Sud, France, 2000 (in french).
8. E. Casarejos, Ph.D. Thesis, University of Santiago de Compostela, Spain, 2001.
9. H. Geissel et al., Ann. Rev. Nucl. Part. Sci. 45 (1995) 163.
10. C.D. Bowman et al., Nucl. Instrum. Methods A 320 (1992) 336.
11. T. Takizuka, Proc. of the International Conference on Accelerator-Driven Transmutation Technologies and Applications, Las Vegas, 1994, edited by E.D. Arthur, A. Rodrigues, and S.O. Schriber (AIP Press, Woodbury, Ny, 1995), p. 64.
12. C. Rubbia et al., CERN report CERN-LHC 96-011-ETT.
13. G. Rossi, Z. Phys. 82 (1933) 151.
14. B.B. Cunningham et al., Phys. Rev. 72 (1947) 739.
15. R. Wolfgang et al., Phys. Rev. 103 (1956) 394.
16. G. Friedlander et al., Phys. Rev. 129 (1963) 1809.
17. H. Sauvageon et al., Z. Phys. A 314 (1983) 181.
18. R. Michel et al., Nucl. Instrum. Methods B 129 (1997) 153.
19. M. Gloris et al., accepted by Nucl. Instrum. Methods. A.
20. H. Geissel et al., Nucl. Instrum. Methods B 70 (1992) 286.
21. P.J. Karol, Phys. Rev. C 11 (1975) 1203.
22. D.J. Morrissey, Phys. Rev. C 39 (1989) 460.
23. A.S. Goldhaber, Phys. Lett. B 53 (1974) 306.
24. M. Hesse et al., Z. Phys. A 355 (1996) 69.
25. J. Benlliure et al., Nucl. Phys. A 660 (1999) 87.